Proceedings of the 2012 IEEE 12th International Conference on Bioinformatics & Bioengineering (BIBE), Larnaca, Cyprus, 11-13 November 2012

Despeckle Filtering in Ultrasound Video of the Common Carotid Artery

Christos P. Loizou[1], Takis Kasparis[2], Pavlos Christodoulides[2], Charoula Theofanous[2], Marios Pantziaris[3], Efthyvoulos Kyriakou[4], Constandinos S. Pattichis[5]

[1]Departement of Computer Science, Intercollege, Limassol, Cyprus, Email: loizou.c@lim.intercollege.a.c.cy
[2]Departement of Electrical Engineering, Computer Engineering & Informatics, Cyprus University of Technology, Limassol, Cyprus, Email: takis.kasparis@cut.ac.cy; paul.christodoulides@cut.ac.cy; ct.theofanous@edu.cut.ac.cy
[3]Institute of Neurology and Genetics, Nicosia, Cyprus, Email: pantzari@cing.ac.cy
[4]Frederick University, Department of Computer Science, Limassol, Cyprus, Email: e.kyriacou@frederick.ac.cy
[5]Departement of Computer Science, University of Cyprus, Nicosia, Cyprus, Email: pattichi@cs.ucy.ac.cy

Abstract—**Noise reduction is essential for increasing the visual quality or as a preprocessing step for further automated analysis in video sequences and video coding. The objective of this work was to investigate four different video despeckle filtering techniques and evaluate them using visual assessment by two medical experts, texture features analysis, and video quality evaluation metrics. The four proposed video despeckle filtering techniques were evaluated on 10 ultrasound videos of the common carotid artery (CCA). The filters were applied on the whole video frame and in a selected by the user region of interest (ROI) which included the atherosclerotic carotid plaque. The despeckle filters were based on linear filtering (DsFlsmv), hybrid median filtering (DsFhmedian), nonlinear filtering (DsFkuwahara) and speckle reducing anisotropic diffusion (DsFsrad) filtering. Our results showed that, the best video despeckle filtering methods were the linear filter DsFlsmv, followed by the hybrid median filter DsFhmedian. Both filters improved the visual perception evaluation by experts and gave better texture and video quality metrics. Further work on a larger number of videos and by employing additional despeckle filtering techniques is required for the evaluation of video despeckle filtering methods on ultrasound videos of the CCA.**

Keywords-Despeckling; video; carotid artery; texture analysis

I. INTRODUCTION

Despite significant progress made in the last few years and the vast technological advancements in image and video processing, there are a number of factors that negatively influence the visual quality of videos and hinder the automated analysis [1]. These include video acquisition technologies, imperfect instruments, natural phenomena, transmission errors, and coding artifacts, which degrade the quality of video data by inducing noise [2]. Ultrasound imaging is a non-invasive powerful diagnostic tool in medicine, but it is degraded by a form of multiplicative noise (speckle), which makes the observation difficult [2]. It is therefore, essential to investigate new filtering techniques for video despeckling.

In this paper, we consider the problem of filtering multiplicative noise (speckle) in ultrasound videos of the common carotid artery (CCA) in order to increase the visual interpretation by experts and facilitate the automated analysis of the videos. The objective of this study was to apply four different video despeckle filtering techniques and to investigate their performance on 10 ultrasound videos of the CCA. The despeckling filtering techniques were evaluated through visual perception evaluation, performed by two medical experts as well as through a number of texture characteristics and video quality metrics. These were extracted from the original and the despeckled videos.

There are several studies reported in the literature for filtering additive noise from natural video sequences [3]-[10], but we have found no other studies where despeckle filtering on ultrasound medical videos (of the CCA) was investigated. Previous research on the use of despeckle filtering of the CCA images was also reported by our group in [2], [11], [12], where improved results were presented in terms of visual quality and classification accuracy between asymptomatic and symptomatic plaques. Moreover, it should be mentioned that a significant number of studies investigated different despeckle filters in various medical ultrasound video modalities with very promising results [2].

The structure of the paper is as follows: In section II, the theoretical concepts of the proposed video despeckle filters are presented. In section III we provide information for the materials and methods used in this study, whereas in section IV we present the results of this study. Sections V and VI present a discussion in relation to previous results from other studies, and the concluding remarks respectively.

II. VIDEO DESPECKLE FILTERS

In this section, the theoretical background for the following four video despeckle filtering methods is introduced: a) linear despeckle filter (DsFlsmv), b) hybrid median filter (DsFhmedian), c) nonlinear filter (DsFkuwahara), and d) speckle reducing anisotropic diffusion (DsFsrad) filtering. Further algorithmic implementation details, and coding can be found in [2]. These filters were applied to each video frame: a) for the whole video frame, and b) for a region of interest (ROI) in each video. The number of iterations, the filtering window size and other filtering parameters that are used for each despeckle filtering method were tuned based on the subjective despeckled video evaluation by two medical experts (see also section III.D).

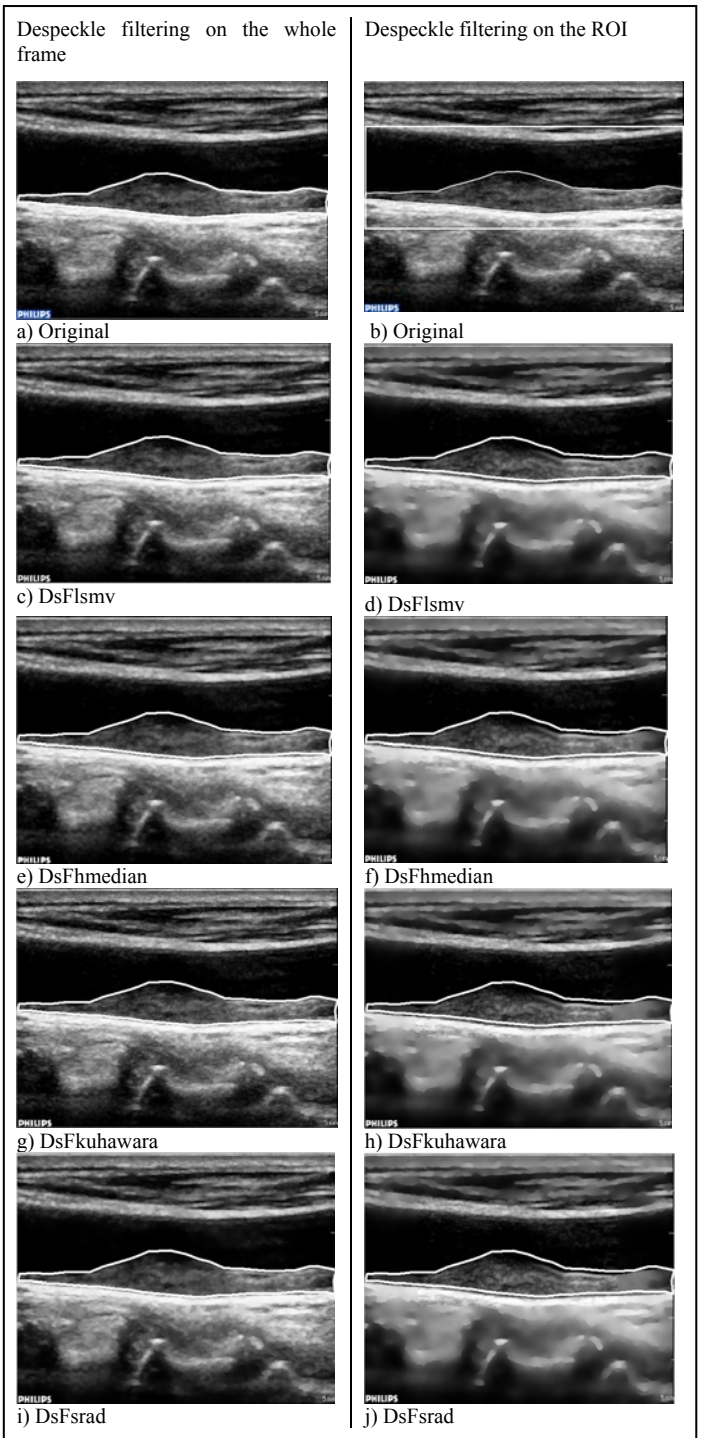

Figure 1. Examples of despeckle filtering on a video frame of a symptomatic CCA video for the whole image frame in the left column, and on an ROI (including the plaque (shown in b)), in the right column for: a), b) original, c), d) DsFlsmv, e), f) DsFhmedian, g), h) DsFkuwahara, and i), j) DsFsrad. The automated plaque segmentations are shown in all examples.

A. Linear Despeckle Filter (DsFlsmv)

The filters of this type utilize the first order statistics such as the variance and the mean of a pixel neighbourhood and may be described with a multiplicative noise model [11]-[13]. Hence the algorithms in this class may be traced back to the following equation:

$$f_{i,j} = \bar{g} + k_{i,j}(g_{i,j} - \bar{g}) \tag{1}$$

where $f_{i,j}$, is the estimated noise-free pixel value, $g_{i,j}$, is the noisy pixel value in the moving window, $\bar{g}$, is the local mean value of an $N_1 \times N_2$ region surrounding and including pixel $g_{i,j}$, $k_{i,j}$ is a weighting factor, with $k \in [0,1]$, and i, j are the pixel coordinates. The factor $k_{i,j}$, is a function of the local statistics in a moving window and is defined [11]-[13] as:

$$k_{i,j} = \frac{(1 - \bar{g}^2\sigma^2)}{(\sigma^2 + \sigma_n^2)}. \tag{2}$$

The values σ^2, and σ_n^2, represent the variance in the moving window and the variance of noise in the whole video frame respectively. The noise variance may be calculated for the logarithmically compressed frame by computing the average noise variance over a number of windows with dimensions considerable larger than the filtering window [11]-[13]. The moving window size for the despeckle filter DsFlsmv was 5x5 and the number of iterations applied to each video frame was two.

B. Hybrid Median Filtering (DsFhmedian)

DsFhmedian, was introduced in [14] and computes the average of the outputs generated by median filtering with three different windows (cross shape window, x-shape window and normal window). A 5x5 size moving window was used with the number of iterations applied to each video frame equal to two.

C. Nonlinear Filtering (DsFkuwahara)

The DsFkuwahara is an 1D filter operating in a 5x5 pixel neighborhood by searching for the most homogenous neighborhood area around each pixel [2], [15]. The middle pixel of the 1x5 neighborhood is then substituted with the median gray level of the 1x5 mask. The filter was iteratively applied two times on the video frame.

D. Speckle Reducing Anisotropic Diffusion Filtering (DsFsrad)

Speckle reducing anisotropic diffusion is described in [16]. It is based on setting the conduction coefficient in the diffusion equation using the local frame gradient and the frame Laplacian. The DsFsrad speckle reducing anisotropic diffusion filter [16] uses two seemingly different methods, namely the Lee [13] and the Frost diffusion filters [17]. A more general updated function for the output image by extending the PDE versions of the despeckle filter is [2], [16]:

$$f_{i,j} = g_{i,j} + \frac{1}{\eta_s} div(c_{srad}(|\nabla g|)\nabla g_{i,j}). \tag{3}$$

where η_s is the size of the filtering window. The diffusion coefficient for the speckle anisotropic diffusion, $c_{srad}(|\nabla g|)$, is derived [16] as:

$$c^2_{srad}(|\nabla g|) = \frac{\frac{1}{2}|\nabla g_{i,j}|^2 - \frac{1}{16}(\nabla^2 g_{i,j})^2}{(g_{i,j} + \frac{1}{4}\nabla^2 g_{i,j})^2}. \quad (4)$$

It is required that $c_{srad}(|\nabla g|) \geq 0$. The above instantaneous coefficient of variation combines a normalized gradient magnitude operator and a normalized Laplacian operator to act like an edge detector for speckle images. High relative gradient magnitude and low relative Laplacian indicates an edge. The DsFsrad filter utilizes speckle reducing anisotropic diffusion after (3) with the diffusion coefficient, $c_{srad}(|\nabla g|)$ in (4) [16]. The coefficient of variation for the DsFsrad filter was 0.015 and the number of iterations was 20.

III. Materials & Methods

A. Recording of Ultrasound Videos

A total of 10 B-mode longitudinal ultrasound videos of the CCA bifurcation were recorded representing different types of atherosclerotic plaque formation with irregular geometry typically found in this blood vessel. The videos were acquired by the ATL HDI-5000 ultrasound scanner (Advanced Technology Laboratories, Seattle, USA) [18] and were recorded digitally on a magneto optical drive, with a resolution of 576x768 pixels with 256 gray levels, and having a frame rate of 100 frames/sec. All video frames were manually resolution-normalized at 16.66 pixels/mm. This was carried out to overcome the small variations in the number of pixels per mm of image depth (i.e for deeply situated carotid arteries, image depth was increased and therefore digital image spatial resolution would have decreased) and in order to maintain uniformity in the digital image spatial resolution [19]. The videos were recorded at the Saint Mary's Hospital, Imperial College of Medicine, Science and Technology, UK from symptomatic subjects at risk of atherosclerosis, which have already developed clinical symptoms, such as a stroke or a transient ischemic attack (TIA). The video despeckling methods were performed for 3-5 seconds intervals, covering in general 2-3 cardiac cycles.

B. Ultrasound Video Normalization

Brightness adjustments of ultrasound videos were carried out in this study based on the method introduced in [20], which improves image compatibility by reducing the variability introduced by different gain settings, different operators, different equipment, and facilitates ultrasound tissue comparability [19]. Algebraic (linear) scaling of the first video frame was manually performed by linearly adjusting the image so that the median gray level value of the blood was 0-5, and the median gray level of the adventitia (artery wall) was 180-190 [20]. The scale of the gray level of the video frames ranged from 0-255. Thus the brightness of all pixels in the video frame was readjusted according to the linear scale defined by selecting the two reference regions. The subsequent frames of

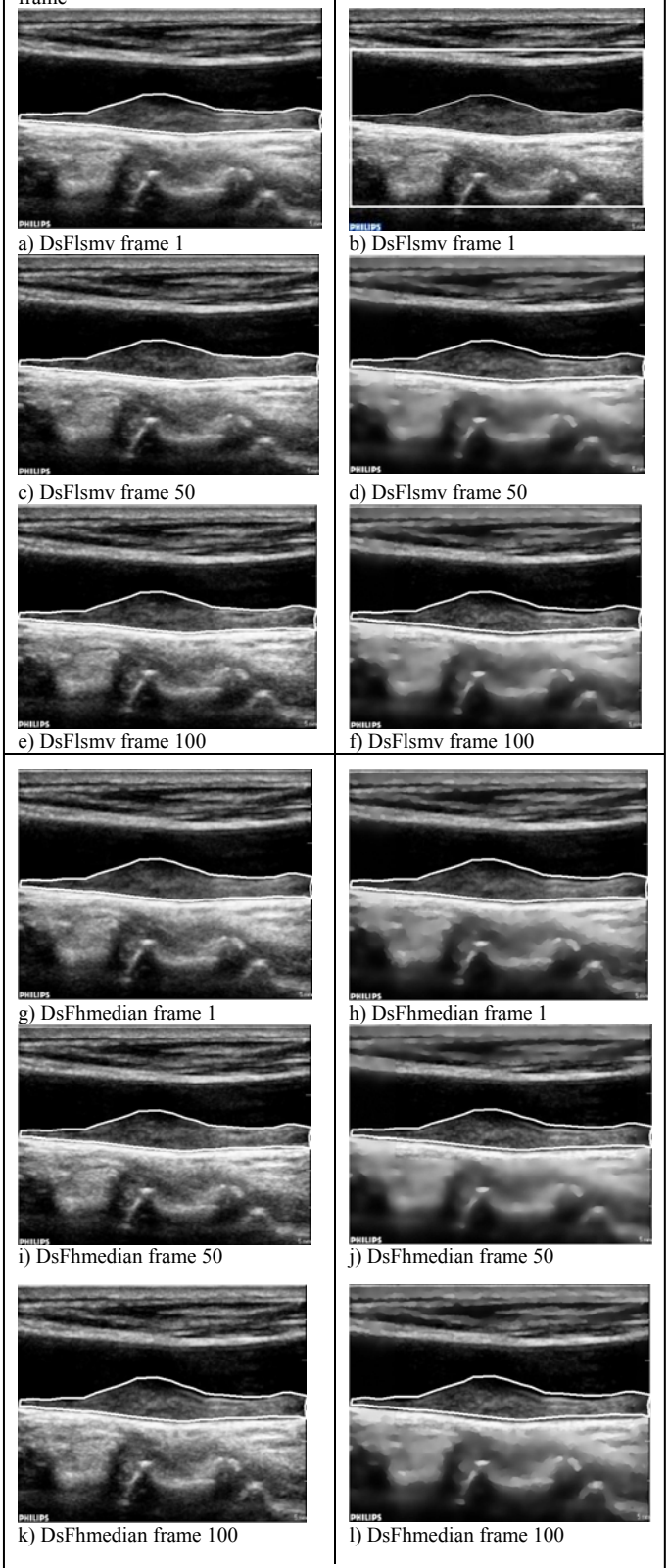

Figure 2. Examples of despeckle filtering with the filter DsFlsmv (a-f) and DsFhmedian (g-l) on a symptomatic video of the CCA with plaque at the far wall of the CCA on frames 1, 50 and 100 for the whole image frame in the left column, and on an ROI (shown in b)), in the right column. The automated plaque segmentations are shown in all examples.

the video were then normalized based on the selection of the first frame.

C. Despeckle filtering

Despeckle filtering was applied to the whole image frame of the video (see Fig. 1, left column) as well as to an ROI selected by the user (see Fig.1, right column). In the latter case the areas outside of the ROI were blurred using the DsFsrad filter with 100 iterations and a coefficient of variation 0.05.

D. Visual Evalution by Experts

The 10 ultrasound videos of the CCA were evaluated visually by two vascular experts, a cardiovascular surgeon, and a neurovascular specialist before and after despeckle filtering. For each case, the original and the despeckled videos (despeckled with filters DsFlsmv, DsFhmedian, DsFKuwahara, DsFsrad) were presented without labeling at random to the two experts. The experts were asked to assign a score in the one to ten scale corresponding to low and high subjective visual perception criteria. Ten was given to a video with the best visual perception. Therefore the maximum score for a filter is 100, if the expert assigned the score of five for all the 10 video. For each filter, the score was divided by ten to be expressed in percentage format. The experts were allowed to give equal scores to more than one video in each case. For each class and for each filter the average score was computed.

The two experts evaluated the area around the distal CCA, 2-3 cm before the bifurcation and the bifurcation for the case where filtering was applied to the whole video frame and for the ROI. It is known that measurements taken from the far wall of the carotid artery are more accurate than those taken from the near wall [20]. Furthermore, the experts were examining the image in the lumen area, in order to identify the existence of a plaque or not.

E. Texture Feature Analysis

Texture provides useful information for the characterization of the atherosclerotic carotid plaque in both images and videos of the CCA [21]. In this study a total of 18 different texture features were extracted both from the original and the despeckled video frames as follows [21]:

(i) Statistical Features (SF): 1) Mean, 2) Median, 3) Variance (σ^2), 4) Skewness (σ^3), and 5) Kurtosis (σ^4). (ii) Spatial Gray Level Dependence Matrices (SGLDM) as proposed by Haralick et al. [22]: 1) Angular second moment, 2) Contrast, 3) Correlation, 4) Sum of squares: variance, 5) Inverse difference moment, 6) Sum average, 7) Sum variance, 8) Sum entropy, 9) Entropy, 10) Difference variance, 11) Difference entropy, 12), and 13) Information measures of correlation.

As texture features data were not normally distributed, the Wilcoxon rank sum test, which calculates the difference between the sum of the ranks of two independent samples, was used in order to identify if for each set of measurements a significant difference (S) or not (NS) exists between the extracted texture features from the original and the despeckled frames, with a confidence level of 95% ($p<0.05$).

F. Video Quality Metrics

Objective video quality assessment is an emerging area of active research [6]. This is very different than image quality assessment that has seen significant growth and success over the last five years. Important video quality metrics, which are also investigated in this study include: a) structural similarity index (SSI), b) visual signal-to-noise ratio (VSNR), c) information fidelity (IFC), d) noise quality measure (NQM), e) weighted signal-to-noise ratio (WSNR) and f) Peak signal-to-noise ratio (RSNR). We refer to [23] for algorithmic details and implementation. The above video quality metrics were calculated from the original and the despeckle video frames.

IV. Results

The performance of the proposed video despeckle filtering methods was evaluated after video normalization and despeckle filtering using visual perception evaluation, texture features, and image quality evaluation metrics. Figure 1 presents the frame 100 of a symptomatic video for the original and the despeckled frames with filters DsFlsmv, DsFhmedian, DsFkuwahara, and DsFsrad when applied to the whole frame (left column) and on an ROI selected by the user of the system (right column) respectively. The automated plaque segmentations performed by an integrated system proposed in [24] are also shown in the images. The filters DsFlsmv and DsFhmedian smoothed the video frame without destroying subtle details. Figure 2 presents the application of the DsFlsmv (see Fig. 2 a-f) and the DsFhmedian (see Fig. 2 g-l) despeckle filters, which showed best performance (see Tables I-III), on consecutive video frames (1, 50 and 100) of a symptomatic subject, for the cases where the filtering was applied on the whole video frame (see left column of Fig. 2) and on an ROI selected by the user (see right column of Fig. 2).

A. Visual Evalution by Experts

Table I presents the results of the visual evaluation of the original and despeckled videos made by the two experts, a cardiovascular surgeon (Expert 1) and a neurovascular specialist (Expert 2). The evaluation was performed on both the whole despeckle video frame as well as to the ROI, where both methods gave similar visual evaluation scorings. The last two rows of Table I present the overall average percentage (%) score assigned by both experts for each filter and the filter ranking. It is shown in Table I that marginally the best video despeckle filter is the DsFlsmv with a score of 74%, followed by the filter DsFhmedian and DsFkuwahara with scores of 73% and 71% respectively. It is interesting to note that the three

TABLE I. PERCENTAGE SCORING OF THE ORIGINAL AND DESPECKLE VIDEOS BY THE EXPERTS.

Experts	***original***	***DsF lsmv***	***DsF hmedian***	***DsF kuwahara***	***DsF srad***
Expert 1	33	75	71	65	61
Expert 2	40	72	75	77	51
Average %	37	74	73	71	56
Ranking	-	1	2	3	4

TABLE II. TEXTURE FEATURES (MEAN±SD), THAT SHOWED SIGNIFICANT DIFFERNCE (USING THE WILCOXON RANK SUM TEST AT $p<0.05$) AFTER DESPECKLE FILTERING, FOR ALL 10 VIDEOS OF THE CCA EXTRACTED FROM THE ORIGINAL AND THE DESPECKLED VIDEOS FROM THE WHOLE VIDEO AND THE ROI (-/-).

Features	*original*	*DsFlsmv*	*DsFhmedian*	*DsFkuwahara*	*DsFsrad*
Median	43±14 / 23±17	43±14 / 28±18	43±14 / 26±12	42±14 / 26±17	43±14 / 26±14
Variance	54±7 / 58±8	53±6 / 58±9	54±6 / 58±8	55±8 / 59±9	54±6 / 62±8
SOV	8±6 / 7±4	12±11 / 9±3	8±7 / 14±22	11±7 / 7±5	10±9 / 12±13
IDM	0.27±0.07 / 0.29±0.14	0.29±0.07 / 0.43±0.09	0.39±0.05 / 0.48±0.09	0.41±0.07 / 0.51±0.089	0.38±0.06 / 0.38±0.094
Entropy	7.8±0.5 / 7±0.96	7.7±0.4 / 6.7±0.9	7.5±0.4 / 6.6±0.9	7.5±0.6 / 6.6±1.1	7.4±0.5 / 7.01±0.8
DE	0.74±0.15 / 0.9±0.2	0.74±0.12 / 0.77±0.15	0.69±0.12 / 0.74±0.13	0.7±0.11 / 0.72±0.1	0.61±0.09 / 0.56±0.16
Coarseness	38±7 / 61±11	93±13 / 110±22	52±10 / 84±21	37±4 / 55±12	54±22 / 33±18

IQR: Inter-qurtile range, SOV: Sum of squares variance,, IDM: Inverse difference moment, DE: Difference entropy

TABLE III. VIDEO QUALITY METRICS (MEAN±SD) FOR ALL 10 VIDEOS OF THE CCA EXTRACTED BETWEEN THE ORIGINAL AND THE DESPECKLED VIDEOS FROM THE WHOLE VIDEO AND THE ROI (-/-).

Features	*DsFlsmv*	*DsFhmedian*	*DsFkuwahara*	*DsFsrad*
SSI	0.98±0.01 / 0.98±0.05	0.97±0.001 / 0.96±0.06	0.77±0.025 / 0.84±0.03	0.96±0.025 / 0.88±0.08
VSNR	36±3.77 / 41±3.0	30±1.86 / 38±5.3	15±1.1 / 24.7±2.3	37±5.7 / 32±10
IFC	7.2±0.93 / 6.2±0.98	6.1±0.6 / 4.6±1.3	1.9±0.08 / 1.4±0.21	6.6±2.3 / 3.7±2.1
NQM	35.3±1.9 / 29±1.9	34±1.4 / 26.7±5.1	17.7±1.1 / 14.2±1.3	34.8±4.9 / 24.1±6.7
WSNR	34.8±1.8 / 38±0.91	33.1±1.1 / 35±5.4	18.8±0.9 / 20.6±1.3	39.1±5.2 / 25±8
PSNR	39.6±2.1 / 42.9±1.6	38.9±1.1 / 40.1±4.5	29.1±1.1 / 29.9±1.2	43.9±4.3 / 34.9±6.9

SSI: Structural similarity index, VSNR: Visual signal-to-noise radio, IFC: Information fidelity criterion, NQM: Noise quality measure, WSNR: Weighted signal-to-noise ratio, PSNR: Peak signal to noise ratio.

filters, DsFlsmv, DsFhmedian and DsFkuwahara, were scored with high evaluation markings by both experts. The filter DsFsrad gave poorer performance with an average score of 56%.

B. Texture Features Analysis

Table II presents the results of selected statistical features (from the SF and SGLDM feature sets, see section III.E), that showed significance difference after despeckle filtering ($p<0.05$). The features were extracted from the original video frame and the despeckled video frames for the whole video frame and the ROI, for all 10 videos investigated in this study. These features were the median, variance, SOV, IDM, entropy, DE and coarseness. It is shown that the filters DsFlsmv and DsFhmedian comparatively preserved the features median, variance and entropy but increased coarseness. It should be noted that these findings cannot be compared with the results presented in references [11], and [12], as the texture features in these two studies were computed for the DsFlsmv despekled plaque images (and not the ROIs as defined in this study).

C. Video Quality Metrics

Table III tabulates selected video quality metrics between the original and the despeckled videos for the whole frame filtering and when the filtering was applied on an ROI. It is clearly shown that the despeckle filter DsFlsmv performs better in terms of quality evaluation for the metrics SSI, VSNR, IFC, NQM, and WSNR when applied on the whole frame. Moreover, all the investigated evaluation metrics gave better results when the DsFlsmv was applied only on the ROI, followed by the DsFhmedian.

V. DISCUSSION

In this work we evaluated four different video despeckling filtering techniques and applied them on 10 ultrasound videos of the CCA. Our effort was to achieve multiplicative noise reduction in order to increase visual perception by the experts but also to make the videos suitable for further analysis such as video segmentation and coding. The video despeckle results were evaluated based on visual perception evaluation by two experts (see Table I), different texture descriptors (see Table II) and video quality metrics (see Table III). The results from (Table I-Table III) as well as the visual evaluation results presented in Fig. 1 and Fig. 2, showed that the best filtering method for ultrasound videos of the CCA is the DsFlsmv followed by the despeckle filter DsFhmedian. Both filters performed best with respect to the visual evaluation by the experts as well as by the video quality metrics. It is noted that the evaluation performance for the DsFlsmv was slightly better. The results of this study are also consistent with our

previous despeckle filtering results found in other studies performed by our group [2], [11], [12] on ultrasound images of the CCA, where the DsFlsmv filter was also found to be the preferred filter in terms of optical perception evaluation and classification accuracy between asymptomatic and symptomatic plaques [11], [12].

While there are a number of despeckle filtering techniques proposed in the literature for despeckle filtering on ultrasound images of the CCA [11]-[17], we have found no other studies in the literate for despeckle filtering in ultrasound videos of the CCA. A it has been mentioned in the introduction a number of studies investigated additive noise filtering in natural video sequences [3]-[10]. The usefulness of these methods in ultrasound video denoising of multiplicative noise still remains to be investigated.

VI. Concluding Remarks

Despeckle filtering is an important operation in the enhancement of ultrasonic video of the carotid artery. Initial findings show some promise of these techniques, however more work is needed to evaluate further the performance of the suggested despeckle filters. Future work wii investigate the application of the above video despeckle filtering methods in a larger video dataset, as well as between asymptomatic and symptomatic patients in order to select the most appropriate filleting method for the two different classes. Furthermore, the proposed despeckle filtering techniques will be investigated and evaluated as a preprocessing step in CCA automated ultrasound video segmentation and in a mobile health telemedicine system. We conjecture that despeckle filtering may favor gain in video transmission.

Acknowledgment

This work was partially funded by the Cyprus University of Technology under the contract named TILEPISKOPISI.

References

[1] Z. Wang, A. Bovik, H. Sheikh, and E. Simoncelli, "Image quality assessment: From error measurement to structural similarity," *IEEE Trans. Image Process.*, vol. 13, no. 4, pp. 600–612, Apr. 2004.

[2] C.P. Loizou and C.S. Pattichis, "Despeckle filtering algorithms and Software for Ultrasound Imaging", Synthesis Lectures on Algorithms and Software for Engineering, Ed. Morgan & Claypool Publishers, San Rafael, CA, USA, 2008.

[3] V. Zlokolica, W. Philips, van de Ville, "Robust non-linear filtering for video processing," *IEEE Proc. Vision, Image and Signal Proces.*, vol. 2, no.2, pp. 571-574, 2002.

[4] T.W. Chan, O.C. Au, T.S. Chong, W.S. Chau, "A novel content-adaptive video denoising filter, *IEEE Proc. Vision, Image and Signal Proces.*, vol. 2, no.2, pp. 649-652, 2005.

[5] K. Dabov, A. Foi, K. Egiazarian, "Video denoising by sparse 3D transform-domain collaborative filtering, *Proc. of the 15th Eur. Sign. Proc. Conf.,* pp. 1-5, 2007.

[6] G. Varghese, Z. Wang, "Video denoising using a spatiotemporal statistical model of wavelet coefficients", *IEEE Int. Conf. on Acoustic, Speech and Sign. Proc,* pp. 1257-1260, 2008.

[7] D. Rusanovskyy, K. Dabov, K. Egiazarian, "Moving-window varying size 3D transform-based video denoising", *Proc. of the Int. Workshop on Video Proc. and Quality Metrics,* pp. 1-4, 2006.

[8] V. Zlokolica, A. Pizurica, W. Philips, "Recursive temporal denoising and motion estimation of video", *Int. Conf. on Image Processing,* vol.3 no. 3, pp. 1465-1468, 2008.

[9] C. Lui, W.T. Freeman W.T., "A high-quality video denoising algorithm based on reliable motion estimation", *European Conf. on Computer Vision,* pp. 706-719, 2010.

[10] M. Maggioni, G. Boracchi, A. Foi, K. Engiazarian, "Video denoising, deblocking and enhancement through separable 4-D nonlocal spatiotemporal transforms," *IEEE Trans. Imag. Proc.,* vol. 21, no. 9, pp. 3952-3966, 2012.

[11] C.P. Loizou, C.S. Pattichis, C.I. Christodoulou, R.S.H. Istepanian, M. Pantziaris, and A. Nicoliades, "Comparative evaluation of despeckle filtering in ultrasound imaging of the carotid artery," *IEEE Trans. on Ultras. Feroel. Freq. Contr*., vol. 52, no. 2, pp. 1653-1669, 2005.

[12] C.P. Loizou, C.S. Pattichis, M. Pantziaris, T. Tyllis, A. Nicolaides, "Quality evaluation of ultrasound imaging in the carotid artery based on normalization and speckle reduction filtering," *Med. Biol. Eng. Comput.*," vol. 44, no. 5, pp. 414-426, 2006.

[13] J.S. Lee, "Digital image enhancement and noise filtering by using local statistics," IEEE Trans. Pattern Anal. Mach. Intellig., PAMI-2, no. 2, pp. 165-168, 1980.

[14] A. Nieminen, P. Heinonen, and Y. Neuvo, "A new class of detail-preserving filters for image processing", IEEE Trans. Pattern Anal. Mach. Intell., vol. 9, pp. 74-90, 1987.

[15] M. Kuwahara, K. Hachimura, S. Eiho, and M. Kinoshita, "Digital processing of biomedical images," Plenum. Pub. Corp., pp. 187–203, Ed. K. Preston and M. Onoe, 1976.

[16] Y. Yongjian and S.T. Acton, "Speckle reducing anisotropic diffusion," IEEE Trans. Image Proc., vol. 11, no. 11, pp. 1260–1270, Nov. 2002.

[17] V.S. Frost, J.A. Stiles, K.S. Shanmungan, and J.C. Holtzman, "A model for radar images and its application for adaptive digital filtering of multiplicative noise," *IEEE Trans. Pattern Anal. Mach. Intellig.*, vol. 4, no. 2, pp.157-165, 1982.

[18] A Philips Medical System Company, "Comparison of image clarity, SonoCT real-time compound imaging versus conventional 2D ultrasound imaging," ATL Ultrasound, Report, 2001.

[19] E. Kyriakou, M.S. Pattichis, C. Christodoulou, C.S. Pattichis S. Kakkos, M. Griffin, A. Nicolaides, "Ultrasound imaging in the analysis of carotid plaque morphology for the assessment of stroke," in Plaque Imaging: Pixel to molecular level, ed. J.S. Suri, C. Yuan D.L. Wilson, S. Laxminarayan, IOS press, pp. 241-275, 2005.

[20] T. Elatrozy, A. Nicolaides, T. Tegos, A. Zarka, M. Griffin, and M. Sabetai, "The effect of B-mode ultrasonic image standardization of the echodensity of symptomatic and asymptomatic carotid bifurcation plaque," Int. Angiol., vol. 17, no. 3, pp. 179-186, 1998.

[21] C. Christodoulou, C. Pattichis, M. Pantziaris, and A. Nicolaides, "Texture-Based Classification of Atherosclerotic Carotid Plaques," *IEEE Trans. Medical Imaging*, vol. 22, no. 7, pp. 902-912, 2003.

[22] R.M. Haralick, K. Shanmugam, and I. Dinstein, "Texture Features for Image Classification," *IEEE Trans. Systems, Man., and Cybernetics*, vol. SMC-3, pp. 610-621, Nov. 1973.

[23] Metrix_mux objective video quality assessment software, Available: http://foulard.ece.cornell.edu/gaubatz/metrix_mux/.

[24] C.P. Loizou, C.S. Pattichis, M. Pantziaris, T. Tyllis, A. Nicolaides, "Snakes based segmentation of the common carotid artery intima media," *Med. Biol. Eng. Comput.*," vol. 45, no. 1, pp. 35-49, Jan. 2007.